Anti-TIGIT biomarker study: Inhibition of TIGIT induces loss of T regs from tumors and requires effector function for tumor growth inhibition

#5627

Gretchen Argast, Fiore Cattaruzza, Erwan Le Scolan, Belinda Cancilla, Pete Yeung, Rose Harris, Gilbert O'Young, Reyhaneh Lahmy, Alayne Brunner, Min Wang, Fumiko Axelrod, Jorge Monteon, Jennifer Elechko, Andrew Lam, Ming-Hong Xie, Austin Gurney, John Lewicki, and Ann M. Kapoun
OncoMed Pharmaceuticals, Inc., Redwood City, CA

INTRODUCTION

- The immune checkpoint co-inhibitory receptor TIGIT (T cell immunoreceptor with Ig ITIM domain) is expressed on regulatory T cells (T regs) and on activated CD4$^+$ T, CD8$^+$ T, and NK cells.
- Blocking TIGIT activity with 313R12, an IgG2a anti-TIGIT antibody activates CD8$^+$ and CD4$^+$ T cells and NK cells, resulting in dose-dependent tumor growth inhibition (TGI) in multiple syngeneic mouse models.
- To explore the pharmacodynamics (PD) and mechanism of action of TGI by anti-TIGIT antibodies, we examined the kinetics of immune cell frequency and activation in tumor by flow cytometry, RT-PCR and immunohistochemistry (IHC).
- In order to determine whether effector function is necessary for anti-TIGIT antibody activity, we compared 313R12 with 313R13, an effector function deficient molecule, in CT26.WT tumors.
- To develop biomarkers for anti-TIGIT, we used gene expression analyses to identify anti-TIGIT gene signatures in tumors and blood from multiple syngeneic models.
- We developed multiplexed IHC panels (e.g. TIGIT+CD8, TIGIT+FOXP3) to quantify expression of TIGIT and TIGIT ligand positive immune cells in the tumor and surrounding stroma, and we profiled a panel of 80 human tumors with these panels.

MATERIALS AND METHODS

313R12 is a surrogate rabbit-mouse chimeric IgG2a monoclonal antibody that binds murine TIGIT, produced by Oncomed Pharmaceuticals. 313R13 is a derivative of 313R12 in which a glycosylation site is mutated, resulting in loss of binding to the Fcγ receptor and loss of effector function.

Large established tumors were used for the *in vivo* mouse experiments: female Balb/C for 4T1, CT26.WT, RENCA and EMT6 and C57Bl/6J for MC38. When tumors reached 250 mm^3, mice were randomized into treatment groups and dosed weekly (IgG2a 12.5 mpk, Saline, and 313R12 at 0.1, 0.5, 2.5 or 12.5 mpk). Tumor measurements were performed twice a week. At the termination of the *in vivo* experiments, tumors and blood were harvested and processed for PD biomarker analysis.

Snap frozen tumor samples were processed using the RNeasy Fibrous Tissue Mini Kit and whole blood RNA was isolated using the PAXgene Blood RNA kit. Total RNA from tumors and paired blood samples was isolated and analyzed using Affymetrix Mouse Genome 430 2.0 oligonucleotide microarrays at Almac Diagnostics. Differentially expressed genes were identified using a paired-sample LIMMA analysis of anti-TIGIT treatment vs saline control samples (triplicate) for each of 5 syngeneic mouse tumor models.

For flow cytometry, tumor samples were dissociated into single cell suspension and incubated with antibody cocktails for membrane markers or intracellular cytokines. Prior to staining for the detection of intra-cellular cytokines, cells were stimulated for 4 hours at 37°C in a CO_2 incubator with 50 ng/ml phorbol 12-myristate 13-acetate, 1 µg/ml ionomycin in the presence of Monensin and Brefeldin A. When staining was complete, the cells were fixed with paraformaldehyde 1.6%. Data were acquired and analyzed on a Fortessa X20 flow cytometer using the FACS DIVA software.

Immunohistochemistry (IHC) to quantify TIGIT on FoxP3+ and CD8+ cells in human tumor tissue was performed using the Ventana Discovery Ultra auto-stainer. RT-PCR analysis was performed on the QuantStudio 7 Flex.

Statistical analyses: For all data, results are presented as Mean±SEM, n=6-10 animals per group. For statistical significance in efficacy studies, **, ***, **** indicate P<0.01, 0.001, 0.0001 respectively, vs IgG2a control by two-way ANOVA followed by Dunnett's post test. For analysis of tumor and spleen weights and for flow cytometry analysis, *, **, ***, **** indicate P<0.05, 0.01, 0.001, 0.0001 respectively, vs IgG2a or saline control by one-way ANOVA followed by Dunnett's post test. For RT-PCR analysis, *, ** indicate P<0.05, 0.01 respectively, vs IgG2a control by one-way ANOVA followed by Sidak post test.

RESULTS

Anti-TIGIT treatment shows anti-tumor efficacy in CT26.WT colon model

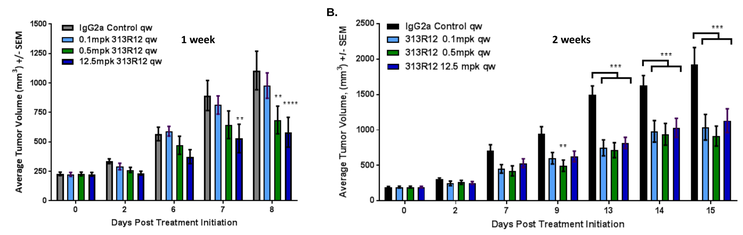

Time course *in vivo* studies performed in the CT26.WT colon carcinoma model using large established tumors with weekly dosing at 0.1, 0.5 and 12.5 mg/kg (mpk) anti-TIGIT. Mice were sacrificed at 24 hours, 7 days and 14 days after the first dose for biomarker analysis. Dose dependent reductions in tumor volumes after one week of dosing are shown in panel A. Panel B shows tumor volume reduction through two weeks' dosing.

Anti-TIGIT decreases T reg frequency in the tumor

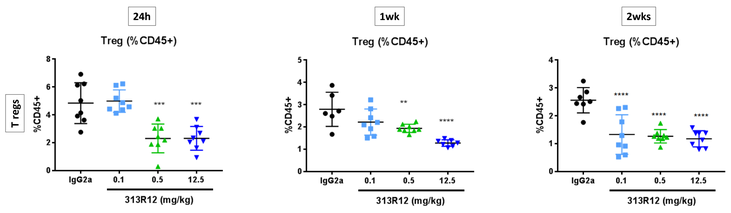

CT26.WT tumors were dissociated and analyzed by flow cytometry. T regs (CD4$^+$, FoxP3$^+$) decreased in the CD45$^+$ cell population after 24 hours of dosing and remained low for up to two weeks. CD8$^+$ cell fractions in the CD45$^+$ population remained consistent over time (data not shown).

Each symbol corresponds to an individual animal. 12.5 mg/kg IgG2a isotype control (black circles), 0.1 mg/kg (mpk) 313R12 (blue squares), 0.5 mg/kg 313R12 (green triangles), 12.5 mg/kg 313R12 (dark blue diamonds).

Anti-TIGIT induces CD226 and cytokine expression in T regs, T cells and NK cells

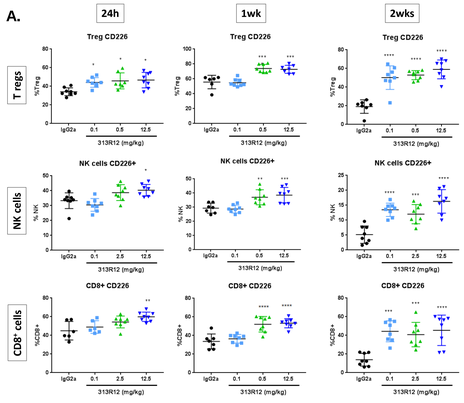

12.5 mg/kg IgG2a isotype control (black circles), 0.1 mg/kg (mpk) 313R12 (blue squares), 0.5 mg/kg 313R12 (green triangles), 12.5 mg/kg 313R13 (dark blue diamonds). Y axis indicates percentage of Treg, NK or CD8$^+$ T cells that were positive for CD226.

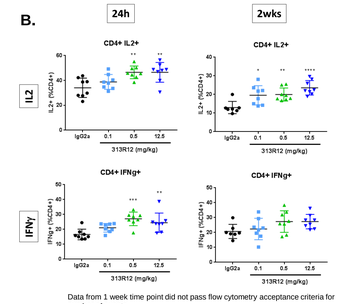

Data from 1 week time point did not pass flow cytometry acceptance criteria for number of events.

CT26.WT mouse tumors were analyzed by flow to detect expression of CD226, a stimulatory receptor in the TIGIT signaling axis, and intracellular cytokine expression in immune cell subtypes over time.

Panel A: Increases in CD226 in tumor immune cells were detected by flow cytometry on T regs, NK cells and T cells after anti-TIGIT treatment in a dose-dependent manner.

Panel B: Intracellular IL2 and IFNγ expression increased in CD4$^+$ T cells with anti-TIGIT treatment at 24 hours and 2 weeks.

Effector function contributes to Anti-TIGIT efficacy

Studies to interrogate effector function-competent 313R12 and effector function-incompetent 313R13 molecules

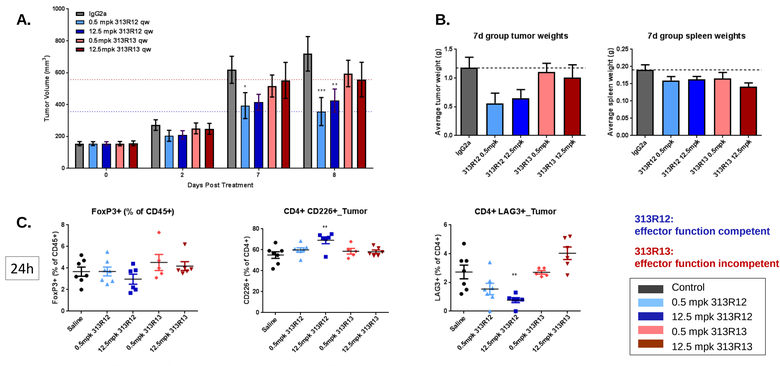

Effector function contributes to efficacy and biomarker changes of anti-TIGIT molecule.

CT26.WT tumor bearing mice were treated with 0.5 or 12.5 mg/kg 313R12 which is effector function competent, or 313R13 which is effector function-incompetent.

Panels A and B: 313R12 treatment resulted in significant TGI compared to 313R13, with minimal effects on spleen weights.

Panel C: Flow cytometry and Panel D: RT-PCR. A greater reduction of T regs in the tumor was observed with 313R12 compared to 313R13. More significant changes were observed with 313R12 compared to 313R13 when comparing effects on immune cell populations, markers of TIGIT signaling axis (CD226), and immune cell activation (Gzma) and exhaustion (Lag3).

Anti-TIGIT Gene signature

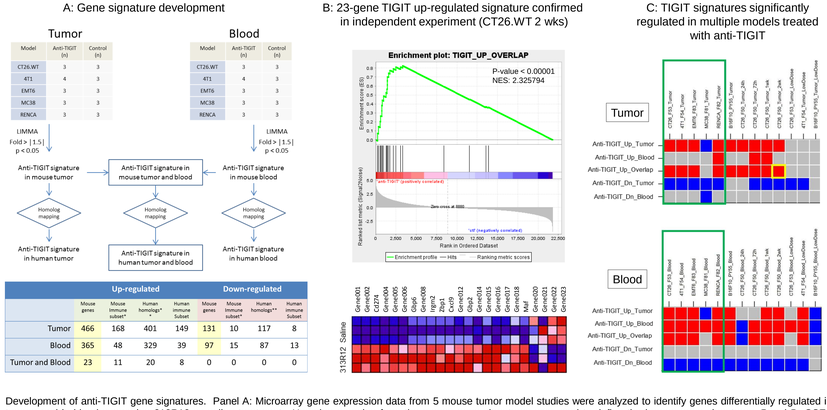

	Up-regulated				Down-regulated			
	Mouse genes	Mouse immune subset*	Human genes	Human immune Subset	Mouse genes	Mouse immune subset*	Human homologs**	Human immune Subset
Tumor	466	168	401	149	131	10	117	8
Blood	365	48	329	39	97	15	87	13
Tumor and Blood	23	11	20	8	0	0	0	0

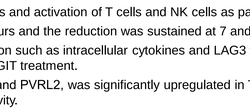

Development of anti-TIGIT gene signatures. Panel A: Microarray gene expression data from 5 mouse tumor model studies were analyzed to identify genes differentially regulated in tumors and in blood comparing 313R12 vs saline treatment. Homolog mapping from the mouse gene signatures was used to define the human gene signatures. Panel B: GSEA analysis confirmed enrichment of the mouse tumor and blood gene signature (23 genes) in an independent mouse experiment. Panel C. GSEA confirmed gene regulation in training and test datasets for 5 mouse anti-TIGIT gene signatures. Summary plot shows significant enrichment of gene signatures up-regulated (red) and down-regulated (blue) at FDR < 5%. Training datasets are shown in the green box. Test datasets included multiple independent models/experiments (n=7). The GSEA analysis from panel C is indicated by the yellow box.

TIGIT expression in immune cells in human tumors by IHC

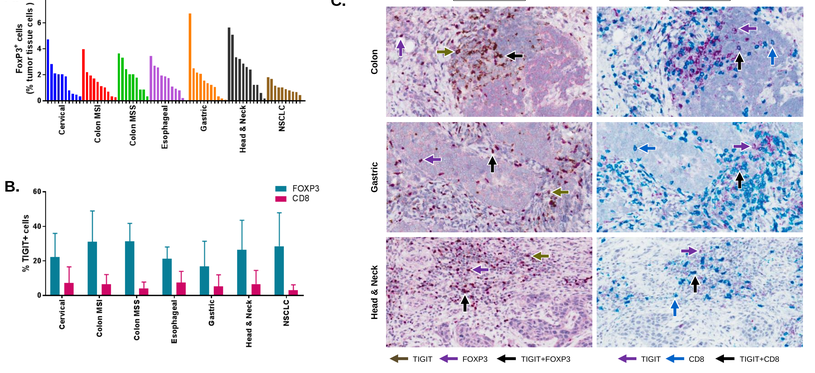

Panel A. Distribution of FOXP3 IHC expression in human tumor tissue (tumor with associated stroma, excluding lymphoid structures) across different tumor types. Panel B. Ratio of TIGIT IHC expression in FOXP3 and CD8 positive cells in human tumor tissue. A larger portion of FOXP3$^+$ cells are also TIGIT positive compare to CD8$^+$, where the majority of cells are TIGIT negative. C. Examples of IHC staining for TIGIT/FOXP3 (brown/purple) and TIGIT/CD8 (purple/teal) in human tumors.

CONCLUSIONS

- Using a surrogate anti-TIGIT antibody, potent single agent dose-dependent anti-tumor efficacy was demonstrated on large established CT26.WT tumors.
- Biomarker analysis demonstrated reduction of T regs and activation of T cells and NK cells as part of the mechanism of action of anti-TIGIT.
  - T regs in the tumor decreased starting at 24 hours and the reduction was sustained at 7 and 14 days.
  - Markers of immune cell activation and exhaustion such as intracellular cytokines and LAG3 were modulated, suggesting a more cytotoxic intratumoral environment after anti-TIGIT treatment.
  - CD226, a co-receptor for TIGIT's ligands PVR and PVRL2, was significantly upregulated in T cells, T regs and NK cells, reflecting a feedback loop activated by inhibiting TIGIT activity.
- Anti-TIGIT requires effector function for tumor growth inhibition. While the effector function-deficient molecule 313R13 was able to induce modest changes in some PD biomarkers including immune cell activation, it required a higher dose than 313R12, and did not result in tumor growth inhibition.
- Anti-TIGIT gene signatures in tumors and in blood were identified from multiple syngeneic models, and have been confirmed using independent experiments.
- In human tumors, TIGIT expression on T regs was found to be considerably higher than on CD8$^+$ T cells by using multiplexed IHC panels (e.g. TIGIT$^+$CD8$^+$ T cells, TIGIT$^+$FOXP3$^+$ T cells) developed to quantify expression of TIGIT and TIGIT ligand-positive immune cells in the tumor and surrounding stroma.